UFSM

CIÊNCIA e NATURA

ISSN 2179-460X
OPEN ACCESS

Ci.e Nat., Santa Maria, v. 45, sp. n. 3, p. 01-17 e75137, 2023 • https://doi.org/10.5902/2179460X75137
Submitted: 03/30/2023 • Approved: 04/10/2023 • Published: 12/01/2023

Special Edition

Computational model verification and numerical analysis of plate buckling due to combined loading

Verificação de modelo computacional e análise numérica de flambagem de placas devido a cargas combinadas

Guilherme Ribeiro Baumgardt[I], Mauro de Vasconcellos Real[I], Paulo Roberto de Freitas Teixeira[I], Elizaldo Domingues dos Santos[I], Thiago da Silveira[II], Liércio André Isoldi[I]

[I] Universidade Federal do Rio Grande, Rio Grande, RS, Brazil
[II] Universidade Federal do Pampa, Alegrete, RS, Brazil

ABSTRACT

Thin plates are structures widely used in different industries due to their mechanical properties. They are often subjected to combined loading, which can cause an undesirable phenomenon called buckling. In this sense, the present work analyzes the elasto-plastic buckling behavior of thin steel plates that are simply supported and subjected to in-plane uniaxial or biaxial compression combined with lateral pressure. To obtain the ultimate stress of the plates, a computational model was developed using the finite element method. Initially, the computational model was verified through previous numerical results from the literature. Then, a case study was carried out considering a rectangular plate geometry with an aspect ratio of b/a = 0.5 (where a and b are the length and width of the plate, respectively) under biaxial compression and varying the lateral loading from 0 to 0.152 MPa, aiming to analyze its elasto-plastic buckling behavior. The results indicated that the computational model was adequately verified. From the case study, it was inferred that the load step plays an important role in the numerical prediction accuracy of the elasto-plastic buckling mechanical behavior of plates. In addition, the application of initial imperfection for small lateral pressures has little influence on ultimate stress, while for larger lateral pressures, it does not generate influence.

Keywords: Elasto-plastic buckling; Thin steel plates; Structural numerical simulation

RESUMO

Placas finas são estruturas amplamente empregadas em diferentes indústrias devido às suas propriedades mecânicas. Elas são frequentemente submetidas a cargas combinadas, que podem causar um fenômeno indesejado chamado flambagem. Nesse sentido, o presente trabalho analisa o

Article published by Ciência e Natura under a CC BY-NC 4.0 license.

comportamento da flambagem elasto-plástica de placas finas de aço, apenas apoiadas, submetidas à compressão uniaxial ou biaxial no plano, combinada com pressão lateral. Para obter a tensão última das placas, foi desenvolvido um modelo computacional através do método dos elementos finitos. Inicialmente, foi realizada a verificação do modelo computacional por meio de resultados numéricos prévios da literatura. Em seguida, foi realizado um estudo de caso considerando uma placa de geometria retangular com razão de aspecto b/a = 0,5 (onde a e b são o comprimento e a largura da placa, respectivamente) submetida à compressão biaxial e variando o carregamento lateral de 0 a 0,152 MPa, visando analisar seu comportamento de flambagem elasto-plástica. Os resultados indicaram que o modelo computacional foi adequadamente verificado. A partir do estudo de caso, inferiu-se que o passo de carga desempenha um papel importante para a precisão da predição numérica do comportamento mecânico da flambagem elasto-plástica de placas. Além disso, a aplicação da imperfeição inicial para pressões laterais pequenas ocasiona pequena influência na tensão última, enquanto para pressões laterais maiores não gera influência.

Palavras-chave: Flambagem elasto-plástica; Placas finas de aço; Simulação numérica estrutural

1 INTRODUCTION

In general, aerospace, naval, and offshore structures are subjected to a combination of two or more types of loads, requiring that the design of these structures consider the interaction among these loads. Due to their mechanical properties, thin plates are widely used in engineering, having an excellent strength-to-weight ratio. These structural components can be subjected to in-plane compression loads, with or without associated lateral (or transverse) loads, which can cause an undesirable phenomenon known as buckling (El-sawy; Nazmy; Martini, 2004). However, according to Soares and Gordo (1996), plates under combined biaxial compressive load and lateral load can lead to a significant reduction in their buckling strength.

Plate buckling can occur in two ways: the first is the elastic buckling, which happens when the plate is slender and the instability takes place in the elastic regime of the material; and the second form is the elasto-plastic buckling, which occurs when the plate reaches the plastic state of the material before the elastic buckling occurrence. As the load increases, the stresses at all points in the plate will increase in the same proportion, and collapse can occur due to loss of strength (Birman, 2011; El-sawy; Nazmy; Martini, 2004).

In this context, the present study aims to verify a finite element computational model (developed in the ANSYS Mechanical APDL software), for the numerical simulation of elasto-plastic buckling of simply supported plates due to combined uniaxial or biaxial in-plane compression and lateral pressure loads. Subsequently, the verified computational model was used to perform a numerical analysis of a rectangular steel plate (with an aspect ratio of b/a = 0.5), subjected to combined loads (biaxial compression and lateral pressure), to evaluate the variation of the ultimate buckling stress behavior of the plate as a result of the increase in transverse load (p_z). For this purpose, three approaches were adopted to properly define the load increments: in the first (case A), an initial number of 100 load steps was defined (resulting in 42.60 N/mm for each step), with a minimum of 50 steps (85.20 N/mm for each step), and a maximum of 200 steps (21.30 N/mm for each load step). In the second (case B), an initial number of 1000 load steps was defined (resulting in 4.26 N/mm for each step), with a minimum of 500 steps (8.52 N/mm for each step), and a maximum of 2000 steps (2.13 N/mm for each load step). Finally, in the third one (case C) the same load step as case B was defined, however the initial imperfection considered in previous cases was not taken into account.

2 COMPUTATIONAL MODEL

The ANSYS Mechanical APDL, which is a commercial software based on the finite element method, was utilized to develop the computational model using the finite element SHELL281. This element was chosen because it is suitable for thin to moderately thick plates. The element has eight nodes with six degrees of freedom at each node: translations in the *x*, *y*, and *z* axes and rotations in the *x*, *y*, and *z* axes, and its formulation is based on the Reissner-Mindlin theory (Ansys, 2017).

According to Wang, Wang and Reddy (2004), for the computational modeling of elasto-plastic buckling of a plate, it is necessary to initially perform the analysis of elastic buckling for the same plate. This is necessary because the configuration of the first mode of elastic buckling is used to define the initial deformed configuration for

the elasto-plastic analysis. The numerical solution through ANSYS® software for plate elastic buckling problems was performed by calculating the eigenvalues. For this type of analysis, according to Madenci and Guven (2015), the equilibrium equations of finite elements are analyzed by solving the homogeneous algebraic equations. The smallest eigenvalue corresponds to the critical buckling load, and the associated eigenvector represents the first mode of buckling. Thus, the global system of equations through the FEM can be written as:

$$[K]\{U\} = \{F\} \tag{1}$$

being [K] the system's stiffness matrix, {F} the force vector, and {U} the vector of unknowns. The force vector, which is normal to the surfaces of each element due to the applied external lateral pressure, can be mathematically described as (Ansys, 2009):

$$\{F\} = \{F_{\mathrm{N}}\} + \{F_{\mathrm{PR}}\} \tag{2}$$

where $\{F_N\}$ is the nodal force applied to each element and $\{F_{PR}\}$ is the pressure vector on each element.

When formulating the plate buckling problem, linear and non-linear terms are considered, obtaining the total stiffness matrix [K], which is determined by the sum of the conventional stiffness matrix for small deformations $[K_E]$, with the geometric stiffness matrix $[K_G]$:

$$[K] = [K_{\mathrm{E}}] + [K_{\mathrm{G}}] \tag{3}$$

being the matrix $[K_G]$ dependent on the geometry and the normal compressive stress $\{\bar{N}_0\}$existing at the beginning of the loading.

In case the load reaches a level of $\{\bar{N}\} = \lambda\{\bar{N}_0\}$, the stiffness matrix is written as:

$$[K] = [K_{\mathrm{E}}] + \lambda[K_{\mathrm{G}}] \tag{4}$$

where λ is a scalar.

Then, the equilibrium equations, governing for the plate, can be written as:

$$\left[[K_{\mathrm{E}}] + \lambda[K_{\mathrm{G}}]\right]\{U\} = \lambda\{\bar{N}_0\} \tag{5}$$

where {U}, the total displacement vector, can be determined by:

$$\{U\} = \left[[K_{\mathrm{E}}] + \lambda[K_{\mathrm{G}}]\right]^{-1}\lambda\{\bar{N}_0\} \tag{6}$$

Przemieniecki (1985) states that in the case of elastic buckling in plates, the structural element being analyzed undergoes significant displacements without any increase in load. Mathematically, the inverse matrix is calculated as the adjoint matrix divided by the determinant of the coefficients. Therefore, the displacements will tend towards infinity when:

$$\det\left[[K_{\mathrm{E}}] + \lambda[K_{\mathrm{G}}]\right] = 0 \tag{7}$$

Solving the eigenvalue problem shown in Eq. (7), the smallest eigenvalue [λ_1] obtained will correspond to the critical buckling load, given by:

$$\{\bar{N}_{\mathrm{cr}}\} = \lambda_1\{\bar{N}_0\} \tag{8}$$

At this point, the load limit is reached and the elastic buckling phenomenon occurs. Additionally, the displacement vector {U} that corresponds to it determines the configuration of the elastic buckling mode (Ansys, 2015).

As plate buckling is not restricted to the material's elastic regime due to its non-linear nature, for the elasto-plastic buckling computational model is crucial to introduce a small initial imperfection value to the plate. In this study, the initial imperfection is determined based on the first elastic buckling mode. This is important because the

post-buckling problem's function does not allow for direct exact analysis, and there are response discontinuities at the neutral equilibrium point. El-Sawy, Nazmy and Martini (2004) found that the most precise results for the ultimate stress of elasto-plastic buckling were achieved when:

$$w_0 = \frac{b}{2000} \tag{9}$$

where w_0 is the value of the initial imperfection and is the plate width.

According to Helbig *et al*. (2016), the ultimate load acting on the plate is given by:

$$P_Y = \sigma_Y t \tag{10}$$

where σ_y is the yield stress of the plate material and *t* is the plate thickness. The Newton-Raphson method is applied to determine the displacements that correspond to the plate equilibrium configuration for each load increment.

According to the findings of Lima *et al*. (2020), at the start of the loading stage $i + 1$, there exists a vector of unbalanced loads $\{\psi\}$that is equivalent to the load increment $\{\Delta\bar{N}\}$, between the vector of external loads $\{\bar{N}\}_{i+1}$ and the vector of non-linear internal forces $\{F_{NL}\}$. This vector is equal to the vector of previous external loads $\{\bar{N}\}_i$. In order to bring down the value of the unbalanced load vector $\{\psi\}$ below the prescribed tolerance level, the Newton-Raphson method is applied iteratively. This is done by utilizing the following equations:

$$\{\psi\} = \{\Delta\bar{N}\} = \{\bar{N}\}_{i+1} - \{F_{NL}\}_r = \{\bar{N}\}_{i+1} - \{\bar{N}\}_i \tag{11}$$

$$\{\psi\}_{r+1} = \{\bar{N}\}_{i+1} - \{F_{NL}\}_r \tag{12}$$

$$\{\psi\}_{r+1} = [K_t]_r\{\Delta U\}_{r+1} \tag{13}$$

$$\{U\}_{r+1} = \{U\}_r + \{\Delta U\}_{r+1} \tag{14}$$

where $\{\psi\}_{r+1}$ is the updated unbalanced load vector, $\{F_{NL}\}_r$ is the nonlinear force vector in the iteration r, $[K]_r$ is the tangent stiffness matrix calculated from the displacement vector $\{U\}_r$, $\{\Delta U\}_{r+1}$ is the updated displacement increment vector, and $\{U\}_{r+1}$ is the updated displacement vector.

Madenci and Guven (2015), Helbig *et al*. (2016) and Lima *et al*. (2020) suggest that failure to achieve convergence in the iterative process during a specific load step signifies the attainment of the ultimate load in the elasto-plastic buckling of the plate.

3 RESULTS AND DISCUSSIONS

Firstly, the verification of the proposed computational model was carried out. Then, using the verified computational model, the case study was conducted.

3.1 Verification of the computational model

To verify the proposed numerical model, a comparison was made with the work of Kumar, Alagusundaramoorthy and Sundaravadivelu (2009), in which it was performed a numerical study of a simply supported stiffened plate with a circular hole subjected to uniaxial compressive load combined with lateral pressure. The numerical simulation was developed considering the stiffened plate of Fig. 1(a), having as computational domain only a portion of the plate with width *b* featuring a stiffener centered on the plate and a circular hole in the center with dimension $d = b/2$, as illustrated in Figs. 1(b) e 1(c). Three values for *b* were evaluated: 170 mm, 340 mm, and 510 mm. In turn, the length of the plate, *a*, and its thickness, *t*, are adopted as 1500 mm and 6 mm, respectively. The angular stiffener has dimensions s = 70 mm, r = 45 mm, and t = 6 mm (see Fig. 1(c)). Moreover, the plate is made of steel with the following mechanical properties: yield strength of σ_y 250 MPa, modulus of elasticity of E = 200 GPa, and Poisson's ratio of ν = 0.3. Regarding the lateral load, different values were applied: 0.114 N/mm², 0.057 N/mm², and 0.038 N/mm²; respectively for the widths of 170 mm, 340 mm, and 510 mm.

Figure 1 – Scheme of the analyzed plate: (a) plate with applied loads, (b) unitary plate, and (c) stiffener dimensions

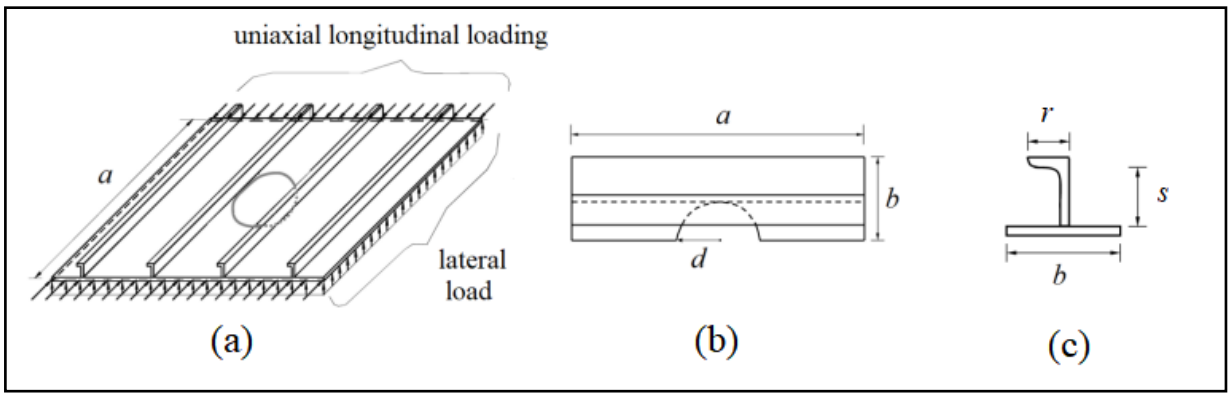

Source: Adapted from Kumar, Alagusundaramoorthy and Sundaravadivelu (2009)

In order to define the spatial discretization to be employed, a thorough mesh convergence test was carried out. It was concluded that the 20 mm element size is the suitable for accurately conducting the numerical simulation for the computational model verification.

The results were obtained by normalizing the ultimate load, which is given by the ratio between the ultimate load of the plate with lateral load, $\overline{N}_{uQ}$, and the ultimate load of the plate without lateral load, $\overline{N}_{u0}$, as shown in Table 1.

Table 1 – Verification of the computational model according to Kumar, Alagusundaramoorthy and Sundaravadivelu (2009)

Width (mm)	$\overline{N}_{uQ} / \overline{N}_{u0}$ **(Present Study)**	$\overline{N}_{uQ} / \overline{N}_{u0}$ **(Kumar et al., 2009)**	**Difference (%)**
170	0.776	0.750	3.48
340	0.803	0.766	4.88
510	0.796	0.766	3.96

Source: Authorship (2023)

It can be observed in Table 1 that the maximum difference obtained was less than 5%, comparing the present study with the results of Kumar, Alagusundaramoorthy and Sundaravadivelu (2009), indicating that the proposed computational model was

adequately verified.

Another verification was carried out based on the work of Yu, Feng and Chen (2015), in which they conducted a numerical study of a simply supported stiffened plate, with a centered square hole, subjected to uniaxial compression combined with a uniformly distributed lateral load, as depicted in Fig 2. Two thickness for the plate were considered: 5 mm and 12 mm; leading to slenderness ratios of 2.45 and 1.02, respectively. The normalized ultimate stress was defined as $\sigma_n = \sigma_u/\sigma_Y$. Moreover, two lateral loads were taken into account: $Q = 2q_u/3$ and $5q_u/6$, where q_u is the ultimate lateral load of the test specimen, which is 341.3 MPa. The studied plates have a length of 1160 mm, a width of 960 mm, and the centered square hole has dimensions of 300 x 300 mm. The angular stiffeners have dimensions $s = 50$ mm, $r = 30$ mm, and $t = 5$ mm (as defined in Fig. 1(c)). The mechanical properties of the steel of the plate are: yield stress of σ_Y 250 MPa, modulus of elasticity of $E = 200$ GPa, and Poisson's ratio of $v = 0.3$. According to the mesh convergence teste performed, a 30 mm element size was used in this numerical simulation.

Figure 2 – Plate with centered square hole: (a) dimensions (in mm), (b) applied loadings

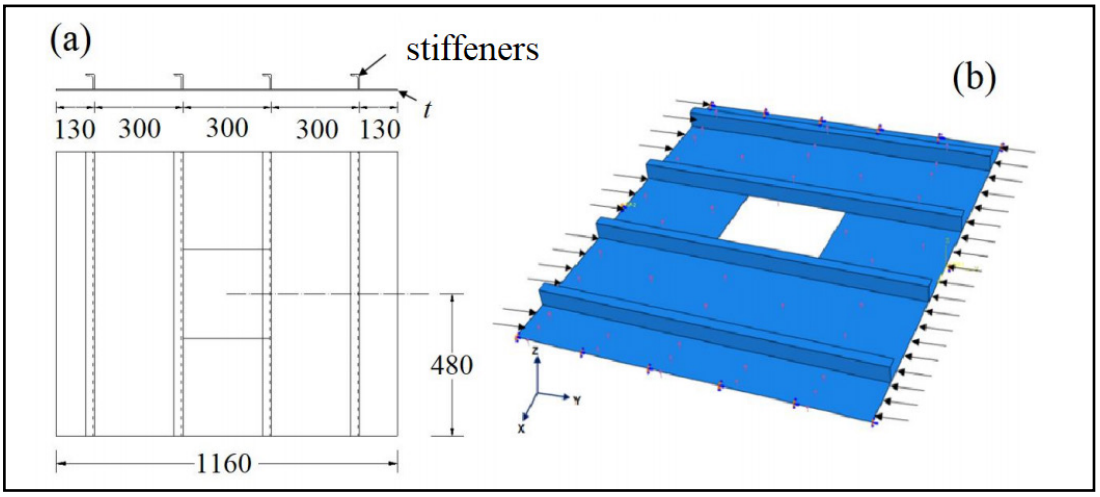

Source: Adapted from Yu, Feng and Chen (2015)

The results obtained in the present study along with the results presented in Yu, Feng and Chen (2015) can be seen in Table 2.

Table 2 – Model verification according to Yu, Feng and Chen (2015)

Thickness (mm)	Lateral load	σ_n (Present Study)	σ_n (Yu et al., 2015)	Difference (%)
5	56	0.335	0.323	3.62
		0.255	0.244	4.64
12	56	0.575	0.591	2.69
		0.565	0.546	3.48

Source: Authorship (2023)

From Table 2, one can note that the maximum absolute difference is less than 5% compared to Yu, Feng and Chen (2015), verifying the proposed computational model.

3.2 Case study

In this case study, the ultimate buckling stress (σ_u) was analyzed for a plate subjected to an in-plane biaxial compressive load combined with a uniformly distributed lateral pressure (p_z) ranging from 0 to 0.152 MPa, for cases A and B, and ranging from 0.005 to 0.152 MPa, for the case C. The plate is simply supported with dimensions of $a = 2000$ mm, $b = 1000$ mm, and $t = 10$ mm, as shown in Fig. 3. The material used was AH36 steel, with properties including an elastic modulus of E 210 GPa, Poisson's ratio of v 0.3, and yield strength of σ_Y 355 MPa. After performing mesh convergence analysis, a finite element size of 30 mm was chosen for this case study.

Figure 3 – Plate with biaxial compressive and lateral load

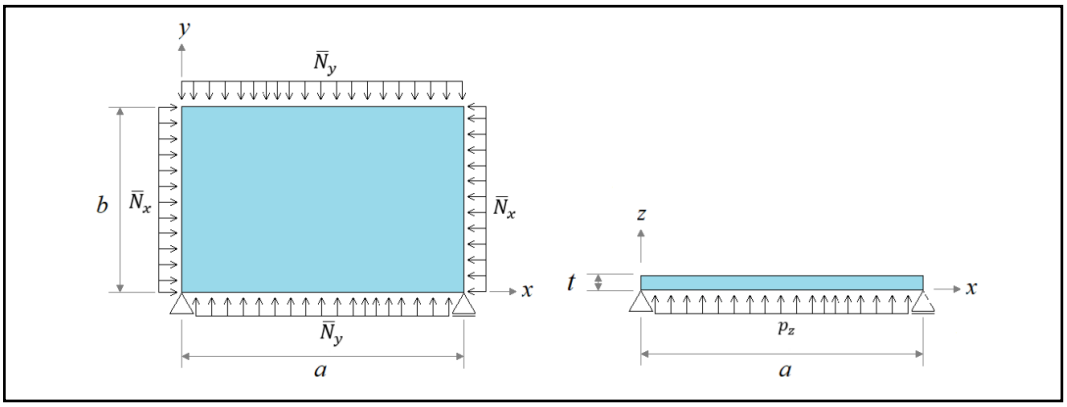

Source: Authorship (2023)

For the case A, an initial number of 100 load steps was defined, resulting in 42.60 N/mm for each step; with a minimum of 50 steps, 85.20 N/mm for each stage; and a maximum of 200 stages, resulting in 21.30 N/mm for each load stage. The results obtained for the case A are presented in Table 3, and it can be observed that, in general, as the lateral pressure increases, the ultimate stress of the plate decreases, as expected. However, one can note plateaus in some lateral pressure intervals, which is an unexpected behavior.

Table 3 – Results obtained for the Case A

Case A					
p_z (MPa)	σ_u (MPa)	p_z (MPa)	σ_u (MPa)	p_z (MPa)	σ_u (MPa)
0.000	50.590	0.051	48.810	0.101	47.040
0.005	50.590	0.056	48.810	0.106	47.040
0.006	50.590	0.061	48.810	0.111	47.040
0.009	49.700	0.066	48.810	0.116	47.040
0.010	49.700	0.071	48.810	0.119	47.040
0.014	49.700	0.076	48.810	0.122	47.040
0.016	49.700	0.079	48.810	0.127	47.040
0.021	49.700	0.083	47.930	0.132	47.040
0.025	49.700	0.084	47.930	0.142	47.040
0.030	49.700	0.085	47.930	0.147	47.040
0.035	49.700	0.086	47.930	0.152	47.040
0.041	49.700	0.091	47.930		
0.046	48.810	0.096	47.040		

Source: Authorship (2023)

The unexpected perceived trend in the case A motivated the realization of case B, in which an initial number of 1000 load steps was defined, resulting in 4.26 N/mm for each step; with a minimum of 500 steps, corresponding to 8.52 N/mm for each step; and a maximum of 2000 stages, resulting in 2.13 N/mm for each load stage. Based on the results obtained, presented in Table 4, a significant reduction in the plateaus identified in case A was observed, thereby achieving an appropriate mechanical behavior.

Finally, for the case C the same load step was applied as for case B, but no initial imperfection was imposed to the plate in this analysis. The results obtained are shown in Table 5 and can be compared with those from case B (see Table 4), indicating that for lower lateral pressures, the initial imperfection influences the ultimate stress (although not significantly), but for higher lateral pressures, there is no difference between the results of cases B and C.

In order to promote a visual comparison among the studied cases, the results of Tables 3, 4, and 5 are plotted in Fig. 4. When comparing case A with cases B and C, it can be observed that by reducing the applied load step, there was a refinement in the obtained results. Therefore, the mechanical behavior for cases B and C is consistent, as the ultimate buckling stress decreases as the lateral pressure increases. Additionally, with the increasing of lateral pressure, the initial imperfection of the plate does not affect the ultimate stress values of the plate, since the results overlap.

Table 4 – Results obtained for the analyzed Case B

Case B					
p_z (MPa)	σ_u (MPa)	p_z (MPa)	σ_u (MPa)	p_z (MPa)	σ_u (MPa)
0.000	50.940	0.051	49.520	0.101	48.280
0.005	50.940	0.056	49.350	0.106	48.100
0.006	50.940	0.061	49.170	0.111	48.100
0.009	50.590	0.066	49.170	0.116	47.930
0.010	50.590	0.071	48.990	0.119	47.930
0.014	50.410	0.076	48.810	0.122	47.930
0.016	50.410	0.079	48.810	0.127	47.750
0.021	50.230	0.083	48.720	0.132	47.570
0.025	50.230	0.084	48.640	0.141	47.390
0.030	50.060	0.085	48.640	0.147	47.300
0.035	49.880	0.086	48.630	0.152	47.220
0.041	49.700	0.091	48.460		
0.046	49.700	0.096	48.460		

Source: Authorship (2023)

Table 5 – Results obtained for the analyzed Case C

Case C					
p_z (MPa)	σ_u (MPa)	p_z (MPa)	σ_u (MPa)	p_z (MPa)	σ_u (MPa)
0.005	50.770	0.051	49.520	0.096	48.460
0.006	50.770	0.056	49.430	0.101	48.280
0.009	50.590	0.061	49.170	0.106	48.100
0.010	50.590	0.066	49.170	0.111	48.100
0.014	50.590	0.071	48.990	0.116	47.930
0.016	50.410	0.076	48.990	0.119	47.930
0.021	50.230	0.079	48.810	0.122	47.930
0.025	50.230	0.083	48.810	0.127	47.750
0.030	50.060	0.084	48.640	0.132	47.570
0.035	49.880	0.085	48.640	0.141	47.390
0.041	49.880	0.086	48.640	0.147	47.300
0.046	49.700	0.091	48.460	0.152	47.220

Source: Authorship (2023)

Figure 4 – Comparison of the results obtained for the three cases analyzed

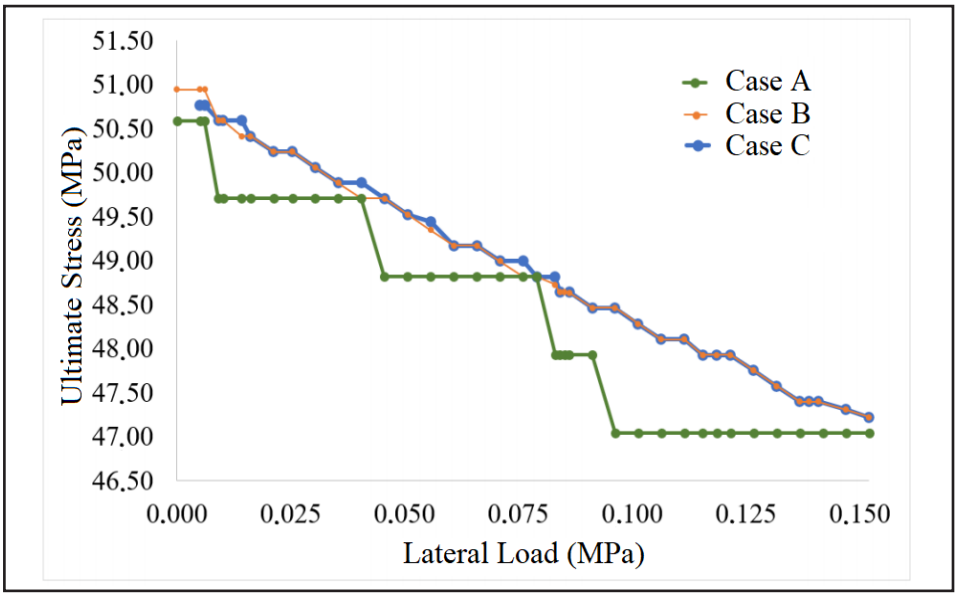

Source: Authorship (2023)

To illustrate how the von Mises stress distribution occurs, the plates with lateral pressure of 0.000, 0.050, 0.101, and 0.152 MPa from Fig. 4 for case B are depicted in Fig. 5.

Figure 5 – Distribution of von Mises stresses on the plate, for case B, under lateral pressure of: (a) 0.000 MPa; (b) 0.050 MPa; (c) 0.101 MPa; and (d) 0.152 MPa

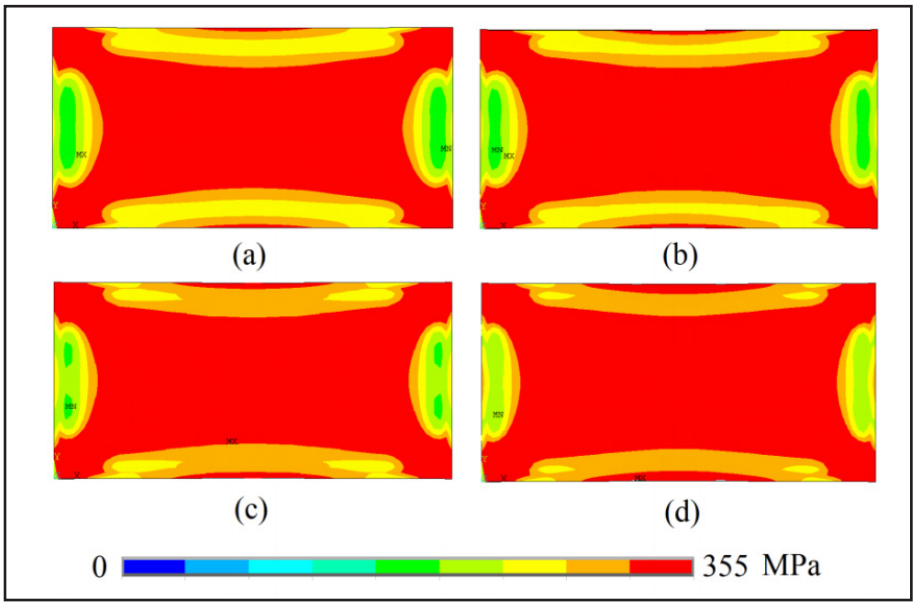

Source: Authorship (2023)

Through Fig. 5, it can be visualized that as the lateral pressure increases, there is an increase in the regions with orange and red colors on the plate, which characterize the highest stresses distributed on the plate. Therefore, the area subjected to the material's limit stress increases as the lateral pressure increases.

4 CONCLUSION

The present work proposed a computational model to numerically simulate the elasto-plastic buckling of plates due to combined loads, developed using the finite element method in ANSYS® software. The computational model was verified against the works of Kumar, Alagusundaramoorthy and Sundaravadivelu (2009) and Yu, Feng and Chen (2015), with a difference of less than 5% in both comparisons, verifying the proposed model.

In the case study, when comparing the results obtained for case A to those of cases B and C, one can infer that it is important to perform a test to identify the adequate

increment of the load step, in order to obtain a physically coherent and accurate solution. Thus, by refining both the mesh and the loading step, the computational effort will increase, increasing the time to perform the analysis.

Regarding the initial imperfection, when comparing the results obtained for cases B and C, it was noticed that the initial imperfection, applied to the numerical model, subtly influences the ultimate stress obtained only for small lateral pressures, and is not necessary for higher lateral pressures.

In future works, it is intended to apply the verified computational model to analyze the influence of the geometric configuration of perforated plates subjected to elasto-plastic buckling due to combined biaxial compressive load and lateral pressure.

ACKNOWLEDGEMENTS

G. R. Baumgardt thanks the *Coordenação de Aperfeiçoamento de Pessoal de Nível Superior* – Brazil (CAPES) for the scholarship of the social demand program (process 88887.501697/2020-00). M.V. Real, P.R.F. Teixeira, E.D. dos Santos, and L.A. Isoldi thank the *Conselho Nacional de Desenvolvimento Científico e Tecnológico* (CNPq) for the research productivity scholarships. All authors thank the Federal University of Rio Grande (FURG) and the Federal University of Pampa (UNIPAMPA).

REFERENCES

ANSYS. **Ansys Help Viewer Release 18.1**. 2017.

ANSYS. **Ansys Mechanical APDL Version 15.0 - User's Guide**. 2015.

ANSYS. **Theory Reference for the Mechanical APDL and Mechanical Applications**. 2009.

BIRMAN, V. **Plates Structures**. Berlim: Springer, 2011. (Solid Mechanics and Its Applications)

EL-SAWY, K. M.; NAZMY, A. S.; MARTINI, M. I. Elasto-Plastic Buckling of Perforated Plates under Uniaxial Compression. **Thin-Walled Structures**, [S. l.], v. 42, n. 8, p. 1083-1101, 2004. Disponível em: https://www.sciencedirect.com/science/article/pii/S0263823104000497?via%3Dihub. Acesso em: 23 fev. 2021.

HELBIG, D. et al. Study about buckling phenomenon in perforated thin steel plates employing computational modeling and constructal design method. **Latin American Journal of Solids and Structures**, São Paulo, v. 13, n. 10, p. 1912-1936, 2016. Disponível em: https://www.scielo.br/j/lajss/a/FL55mFmf3d7yJsGf35jtPgb/?lang=en. Acesso em: 16 nov. 2020.

KUMAR, M.S.; ALAGUSUNDARAMOORTHY, P.; SUNDARAVADIVELU, R. Interaction curves for stiffened panel with circular opening under axial and lateral loads. **Ships and Offshore Structures**, Cambridge, v. 4, n. 2, p. 133–143, 2009. Disponível em: https://www.tandfonline.com/doi/abs/10.1080/17445300902746420. Acesso em: 25 mar. 2021.

LIMA, J. P. S. *et al*. Constructal Design for the ultimate buckling stress improvement of stiffened plates submitted to uniaxial compressive load. **Engineering Structures**, v. 203, 2020. Disponível em: https://www.sciencedirect.com/science/article/pii/S0141029619320292?via%3Dihub. Acesso em:16 nov. 2020.

MADENCI, E.; GUVEN, I. **The Finite Element Method and Applications in Engineering Using ANSYS**. 2. ed. Berlim: Springer, 2015.

PRZEMIENIECKI, J. S. **Theory of Matrix Structural Analysis**. Massachusetts: Courier Corporation, 1985.

SOARES, C. G.; GORDO, J. M. Compressive Strength of Rectangular Plates Under Biaxial Load and Lateral Pressure. **Thin-Walled Structure**, [*S. l.*], v. 24, n. 3, p. 231-259, 1996. Disponível em: https://www.sciencedirect.com/science/article/pii/0263823195000305. Acesso em: 07 jul. 2021.

WANG, C. M.; WANG, C. Y.; REDDY, J. N. **Exact Solutions for Buckling of Structural Members**, Boca Raton, Flórida: CRC Press, 2004. (Computational Mechanics and Applied Analysis, v. 6).

YU, C. L.; FENG, J. C.; CHEN, K. Ultimate uniaxial compressive strength of stiffened panel with opening under lateral pressure. **International Journal of Naval Architecture and Ocean Engineering**, v. 7, n. 2, p. 399-408, 2015. Disponível em: https://www.sciencedirect.com/science/article/pii/S2092678216300887?via%3Dihub. Acesso em: 23 fev. 2021.

Authorship contributions

1 – Guilherme Ribeiro Baumgardt

Graduate Student, MSc
https://orcid.org/0009-0001-4199-190X • guilhermebaumgardt@gmail.com
Contribution: Conceptualization, Methodology, Software, Validation, Data Curation, Formal Analysis, Investigation, Resources, Data Curation, Writing - First Draft , Data Visualization

2 – Mauro de Vasconcellos Real

Professor, Doctor
https://orcid.org/0000-0003-4916-9133 • mvrealgm@gmail.com
Contribution: Conceptualization, Methodology, Validation, Data Curation, Formal Analysis, Investigation, Resources, Data Curation, Data Visualization, Project Management.

3 – Paulo Roberto de Freitas Teixeira

Professor/Doctor
https://orcid.org/0000-0003-0773-6865 • prfreitasteixeira@gmail.com
Contribution:Conceptualization, Methodology, Validation, Data Curation, Formal Analysis, Investigation, Resources, Data Curation, Data Visualization, Project Management.

4 – Elizaldo Domingues dos Santos

Associate Professor/Doctor
https://orcid.org/0000-0003-4566-2350 • elizaldosantos@furg.br
Contribution:Conceptualization, Methodology, Validation, Data Curation, Formal Analysis, Investigation, Resources, Data Curation, Data Visualization, Project Management.

5 – Thiago da Silveira

Professor/Doctor
https://orcid.org/0000-0002-6874-7229 • thiagods@unipampa.edu.br
Contribution: Conceptualization, Methodology, Software, Validation, Data Curation, Formal Analysis, Investigation, Resources, Data Curation, Writing - Revision and Editing, Data Visualization, Supervision, Project Management

6 – Liércio André Isoldi

Professor/Doctor
https://orcid.org/0000-0002-9337-3169 • liercioisoldi@furg.br
Contribution: Conceptualization, Methodology, Validation, Data Curation, Formal Analysis, Investigation, Resources, Data Curation, Writing - Revision and Editing, Data Visualization, Supervision, Project Management

How to quote this article

BAUMGARDT, G. R.; REAL, M. de V.; TEIXEIRA, P. R. de F.; SANTOS, E. D. dos; SILVEIRA, T. da; ISOLDI, L. A. Computational model verification and numerical analysis of plate buckling due to combined loading. **Ciência e Natura**, Santa Maria, v. 45, spe. n. 3, e75137, 2023. DOI: https://doi.org/10.5902/2179460X75137. Available from: https://doi.org/10.5902/2179460X75137. Accessed in: day month abbr. year.